Spin tunnelling dynamics for spin-1 Bose–Einstein condensates in a swept magnetic field

To cite this article: Guan-Fang Wang *et al* 2008 *J. Phys.: Condens. Matter* **20** 045223

View the article online for updates and enhancements.

Spin tunnelling dynamics for spin-1 Bose–Einstein condensates in a swept magnetic field

Guan-Fang Wang[1]**, Li-Bin Fu**[1] **and Jie Liu**[1,2]

[1] Institute of Applied Physics and Computational Mathematics, PO Box 8009 (28),
100088 Beijing, People's Republic of China
[2] Center for Applied Physics and Technology, Peking University, 100084 Beijing,
People's Republic of China

E-mail: Liu_Jie@iapcm.ac.cn

Abstract
We investigate the spin tunnelling of spin-1 Bose–Einstein condensates in a linearly swept
magnetic field with a mean-field treatment. We focus on the two typical alkali Bose atoms ^{87}Rb
and ^{23}Na condensates and study their tunnelling dynamics according to the sweep rates of the
external magnetic fields. In the adiabatic (i.e. slowly sweeping) and sudden (i.e. fast sweeping)
limits, no tunnelling is observed. For the case of moderate sweep rates, the tunnelling dynamics
is found to be very sensitive to the sweep rates, so the plots of tunnelling probability versus
sweep rate only become resolvable at a resolution of 10^{-4} G s^{-1}. Moreover, a conserved quantity
standing for the magnetization in experiments is found to affect dramatically the dynamics of
the spin tunnelling. Theoretically we have given a complete interpretation of the above findings,
and our studies could stimulate the experimental study of spinor Bose–Einstein condensates.

(Some figures in this article are in colour only in the electronic version)

1. Introduction

Bose–Einstein condensation (BEC) has been one of the most active topics in physics for over a decade, and yet interest in this field remains impressively high. One of the hallmarks of BEC in dilute atomic gases is the relatively weak and well-characterized interatomic interactions. The vast majority of theoretical and experimental work has involved single-component systems, using magnetic traps confining just one Zeeman sublevel in the ground-state hyperfine manifold, including the BEC–BCS (Bardeen–Cooper–Schrieffer) crossover [1, 2], quantized vortices [3–5], condensates in optical lattices [6], and low-dimensional quantum gases [7, 8]. An impotent frontier in BEC research is the extension to multicomponent systems, which provides a unique opportunity for exploring coupled, interacting quantum fluids, especially atomic BECs with internal quantum structures. Some experiments have observed spin properties of $f = 1$ and 2 condensates [9–13], using a far-off resonant optical trap to liberate the internal spin degrees of freedom. Even $f = 3$ bosons are also investigated in a present theoretical work [14]. For atoms in the $f = 1$ ground-state manifold, the presence of Zeeman degeneracy and spin-dependent atom–atom interactions [10, 15–20] leads to interesting condensate spin dynamics. Much literature has been devoted to spin mixing and the spin domain, which has been observed in experiments.

In this paper, we investigate spin tunnelling for a spin-1 BEC with a mean-field description. Unlike all previous studies of the fixed external magnetic fields, both in theory and experiment (e.g. see [19–21]), we highlight the important role of an external magnetic field, which is now set to be linearly varying with time. We focus on the two typical alkali Bose atoms ^{87}Rb and ^{23}Na condensates and study their tunnelling dynamics according to different sweep rates of external magnetic fields. We also pay much attention to a conserved quantity, m, standing for magnetization, and find that it can dramatically affect the tunnelling dynamics for both ^{87}Rb and ^{23}Na atom systems.

Our paper is organized as follows. Section 2 introduces our model. In sections 3 and 4 we demonstrate our thorough investigation on the spin tunnelling of Bose atoms ^{87}Rb and ^{23}Na condensates, respectively. Also, theoretical interpretation of the spin tunnelling is given with the help of both analytical deductions and phase space analysis. Section 5 is our conclusion.

2. The model

In an external magnetic field, the spin-1 Bose–Einstein condensate (BEC) is described with by following Hamiltonian [21],

$$H = \int \mathrm{d}r \left[\psi_i^\dagger \left(-\frac{\hbar^2}{2M} \nabla^2 + v + E_i \right) \psi_i + \frac{c_0}{2} \psi_i^\dagger \psi_j^\dagger \psi_j \psi_i \right.$$
$$\left. + \frac{c_2}{2} \psi_k^\dagger \psi_i^\dagger (F_\gamma)_{ij} (F_\gamma)_{kl} \psi_j \psi_l \right], \tag{1}$$

where repeated indices are summed and $\psi_i^\dagger(r)$ (ψ_i) is the field operator that creates (annihilates) an atom in the ith hyperfine state ($|f = 1, i = +1, 0, -1\rangle$, hereafter $|i\rangle$) at location r. M is the mass of an atom. Interaction terms with coefficients c_0 and c_2 describe elastic collisions of spin-1 atoms, expressed in terms of the scattering length a_0 (a_2) for two spin-1 atoms in the combined symmetric channel of total spin 0 (2), $c_0 = 4\pi\hbar^2(a_0 + 2a_2)/3M$ and $c_2 = 4\pi\hbar^2(a_2 - a_0)/3M$. a_0 is not spin concerned. a_2 is spin concerned. $F_{\gamma=x,y,z}$ are spin-1 matrices. Assuming the external magnetic field B to be along the quantization axis ($\hat{z}$), the Zeeman shift on an atom in state $|i\rangle$ becomes [22]

$$E_\pm = -\frac{E_{\mathrm{hf}}}{8} \mp g_I \mu_I B - \frac{E_{\mathrm{hf}}}{2} \sqrt{1 \pm \xi + \xi^2} \tag{2}$$

$$E_0 = -\frac{E_{\mathrm{hf}}}{8} - \frac{E_{\mathrm{hf}}}{2} \sqrt{1 + \xi^2}, \tag{3}$$

where E_{hf} is the hyperfine splitting and g_I is the Lande g factor for an atom with nuclear spin I. μ_I is the nuclear magneton and $\xi = (g_I \mu_I B + g_J \mu_B B)/E_{\mathrm{hf}}$, with g_J representing Lande g factor for a valence electron with a total angular momentum J. μ_B is the Bohr magneton.

At near-zero temperature and when the total number of condensed atoms (N) is large, the system can be well described in the mean-field approximation. For an isotropic Bose gas, under the mean-field method and single model approximation, the operators can be substituted by c numbers $\psi_i = a_i \phi(r)$, where a_i corresponds to the probability amplitudes of atoms in the ith hyperfine state. By setting $a_i = \sqrt{s_i} \mathrm{e}^{\mathrm{i}\theta_i}$, the system can be described by the following classical Hamiltonian system [21],

$$H_{\mathrm{mf}} = E_+ s_1 + E_0 s_0 + E_- s_{-1} - c[(1 - s_1 - s_{-1})^2$$
$$+ 4s_1 s_{-1} - 4(1 - s_1 - s_{-1})\sqrt{s_1 s_{-1}} \cos\theta], \tag{4}$$

where $\theta = \theta_1 + \theta_{-1} - 2\theta_0$ and $c = c_2 \int \mathrm{d}r |\phi(r)|^4$. Using canonically conjugate transformation, H_{mf} can be transferred into the following compact classical Hamiltonian (up to a trivial constant),

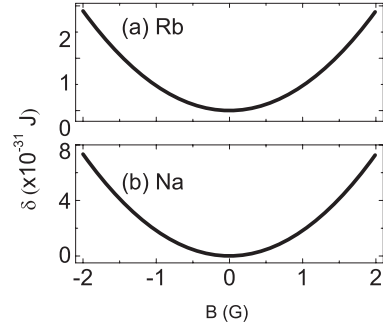$$H_c = 2cs_0 \left[(1 - s_0) + \sqrt{(1 - s_0)^2 - m^2} \cos\theta \right] + \delta(1 - s_0), \tag{5}$$

Figure 1. The transformation of δ, expressed in terms of the Zeeman shift of an atom in state $|i\rangle$ ($i = +1, 0, -1$) in the external magnetic field B with $\mu_I = 5.05 \times 10^{-27}$ J T^{-1}, $\mu_B = 9.274 \times 10^{-24}$ J T^{-1}: (a) for ^{87}Rb atom condensate with $g_I = 1.834$, $g_J = 2$, $E_{\mathrm{hf}} = 6835h(MH_z * J * s)$; (b) for ^{23}Na atom condensate with $g_I = 1.47867$, $g_J = 2$, $E_{\mathrm{hf}} = 1772h(MH_z * J * s)$.

and the equations of motions for canonically conjugate variables s_0, θ are

$$\dot{s}_0 = \frac{4c}{\hbar} s_0 \sqrt{(1 - s_0)^2 - m^2} \sin\theta, \tag{6}$$

$$\dot{\theta} = -\frac{2\delta}{\hbar} + \frac{4c}{\hbar}(1 - 2s_0) + \frac{4c}{\hbar}$$
$$\times \frac{(1 - s_0)(1 - 2s_0) - m^2}{\sqrt{(1 - s_0)^2 - m^2}} \cos\theta, \tag{7}$$

where $m = s_{-1} - s_1$ is conserved and denoted as magnetization, and $\delta = (E_+ + E_- - 2E_0)/2$. Figure 1 shows the relationship between δ and the external magnetic field B for the parameters of the ^{87}Rb and ^{23}Na systems [22], respectively.

3. Spin tunnelling for ^{87}Rb atom condensate

As a spin dynamics problems, spin tunnelling has attracted much attention both theoretically and experimentally. In this section, we study spin tunnelling for the spin-1 BEC system in a swept magnetic field. Because ^{87}Rb atom condensate can readily be prepared in experiments and has been involved in many investigations, we discuss it first.

3.1. Resonance window for spin tunnelling

In our study, the magnetic field varies linearly over time, i.e. $B \sim \alpha t$, where α is the sweep rate. The swept magnetic field is far away from Feshbach resonance so that the atom–atom interaction is almost constant during the sweeping process. In our following calculations, the interval of the magnetic field is set to be $[-B_0, B_0]$ of $B_0 = 2$ G. The B_0 is chosen to be so large that the coupling between different components can be safely ignored at the beginning and the end of the sweep of the magnetic field, and the spin tunnelling probability can be well defined (see figure 2, for example). The initial population for the spin-0 component is supposed s_0^{Initial} (i.e. at $-B_0$), and what we are concerned with is the final population of spin-0 state (i.e. s_0^{Final}) after the external field sweeps from $-B_0$ to B_0. To this end, we exploit the Runge–Kutta 4th–5th algorithm to solve numerically the coupled
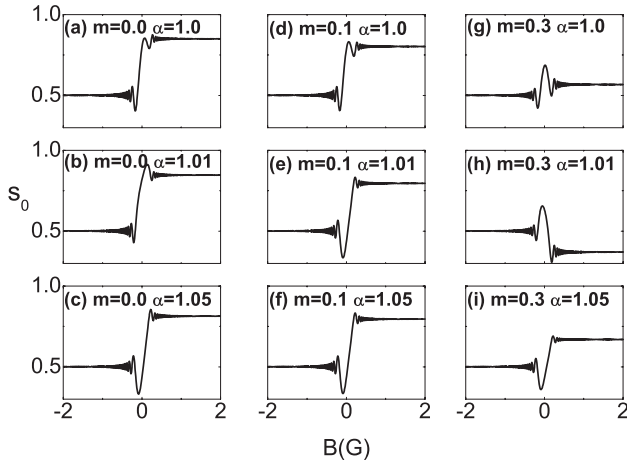
Figure 2. The change in s_0 (its initial value is 0.5 at $B_0 = 2$ G) with the sweep in magnetic field B for ^{87}Rb at $m = 0.0, 0.1, 0.3$, $\alpha = 1.0, 1.01, 1.05$, respectively, and $c = -3.13 \times 10^{-34}$ J.
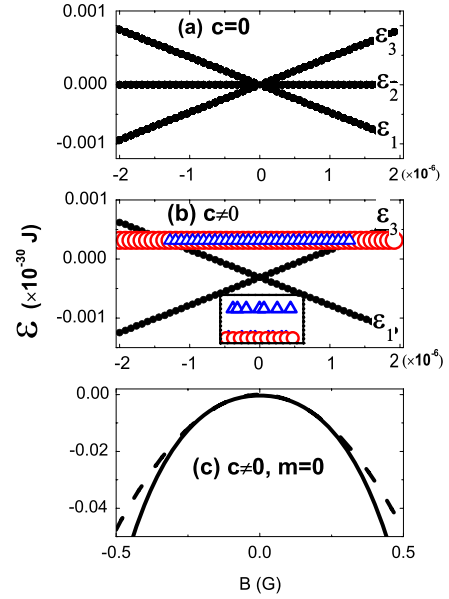

Figure 3. The eigenvalues of ^{87}Rb atom condensate: (a) for $c = 0$ and different m; (b) for $c = -3.13 \times 10^{-34}$ J and different m, where the triangle is ε_{2a} and the circle is ε_{2b} (the inset shows that ε_{2a} and ε_{2b} are non-degenerate); (c) for $c = -3.13 \times 10^{-34}$ J and $m = 0$, where the dashed line is H_{mf1} and the solid line is H_{mf2}. To show the spin tunnelling around $B = 0$ clearly in figure 2, the unit for the horizons of (a) and (b) is taken to be 10^{-6} G, while it is G in (c).

ordinary differential equations (6) and (7) for the parameters corresponding to Bose atoms ^{87}Rb.

For convenience and without loss of generality, we set the initial probability of s_0 to be 0.5 as an example, which corresponds to the lowest energy of the system [21] and can easily be prepared in experiments. The spin tunnelling process can be seen by drawing the evolution of s_0 with respect to instantaneous magnetic fields B. In figure 2, we plot the temporal evolution of s_0 with B for different sweep rates $\alpha = 1.0, 1.01, 1.05$. For each α we choose several magnetization quantities for comparison. It is shown in figure 2 that spin tunnelling happens mainly in a small window around $B = 0$, regardless of the different quantities of magnetization, and the tunnelling processes are very sensitive to the sweep rates. Moreover, we find the conserved magnetization m dramatically affects the tunnelling processes and the final tunnelling probability. For example, as shown in the first row of figure 2, on increasing the magnetization from 0 to 0.3, after a round sweep of the external magnetic field, the occupation population of BEC in the spin-0 component changes from being enhanced to being quenched compared to its initial state.

The crucial effect of the magnetization parameter on spin tunnelling can be understood roughly from equations (6) and (7) such that the variation in the population s_0 is restricted by the conserved magnetization quantity, i.e. $|1 - s_0| > |m|$.

To explain why spin tunnelling happens mainly in a small window around the zero value of the magnetic field, i.e. $B = 0$, we calculate the eigenvalues and the eigenstates of the system by using similar methods to those developed in our recent work [24]. Solving the eigenequations of the system, we obtain the eigenvalues or eigenenergies. Figure 3(a) plots the eigenvalues for the linear case, i.e. $c = 0$, and figure 3(b) for the nonlinear case, i.e. $c \neq 0$. For the linear case, the system has three levels, as shown in figure 3(a). These are $\varepsilon_1 = E_+ + c, \varepsilon_2 = E_0 + c, \varepsilon_3 = E_- + c$ corresponding to $m = -1, 0, 1$, respectively, and they cross at $B = 0$. When $c \neq 0$, the mid-level ε_2 moves up and splits into two levels, i.e. $\varepsilon_{2a} = (E_+ + E_-)/2 - c$ (the triangles in figure 3(b)) and

$\varepsilon_{2b} = E_0 - c$ (the circles in figure 3(b)) corresponding to $m = (E_+ - E_-)/4c$ and $m = 0$, respectively. ε_{2a} corresponds to the states of $s_0 = 0$, while ε_{2b} corresponds to those of $s_0 = 1$. They are seemingly degenerate, while the inset graph in figure 3(b) shows that they are actually non-degenerate. Furthermore, we find an interesting phenomenon for this irregular system through investigating the extreme energies of the classical Hamiltonian. After adding the nonlinearity to the system, these extremes are different from the eigenvalues for the same m. For example, taking $m = 0$, in order to ensure the exact position of the extreme energies, we use H_{mf} and obtain its two extreme values $H_{\mathrm{mf1}} = E_0$ and $H_{\mathrm{mf2}} = \delta/2 + \delta^2/16c + E_0 + c$. These are plotted in figure 3(c). Due to these levels being very close around $B = 0$, tunnelling between these levels occurs easily. Moreover, our calculation reveals that these almost degenerate solutions only emerge in magnetic fields in the range $[-0.16, 0.16]$ G. This means that tunnelling should mainly occur in this regime. The above analysis coincides with the jumping regime of s_0 in figure 2. In this way, we explain why spin tunnelling mainly occurs in a small resonance window around $B = 0$.

3.2. Spin tunnelling probability

In this subsection, by studying the tunnelling probability of ^{87}Rb atom condensate in a swept magnetic field, we find a novel phenomenon. We define this sensitive spin tunnelling.

Because most experimental and theoretical studies are concerned with zero magnetization, we mainly calculate the tunnelling probability for $m = 0.0$. For convenience and without loss of generality, we set the initial probability of s_0
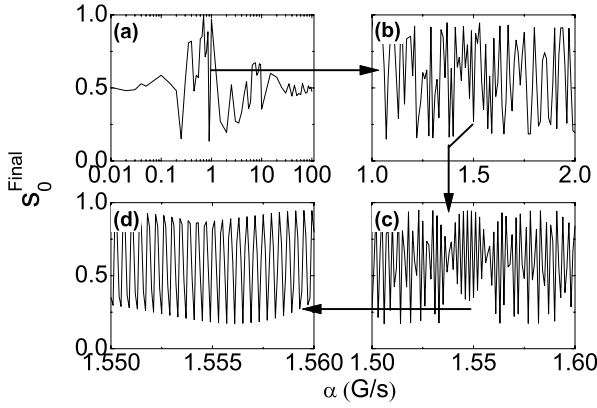
Figure 4. The tunnelling probability of ^{87}Rb atom condensate at $m = 0.0$, $c = -3.13 \times 10^{-34}$ J. (b) is a magnified part of (a) for a moderate sweep rate of magnetic field. (c) is a magnification of (b), and (d) is a magnification of (c).

Figure 5. The relationship between the initial value of s_0 at $B = -2$ G, s_0^{Initial}, and its final value at $B = 2$ G, s_0^{Final}, for $\alpha = 0.01, 0.5, 100$, $m = 0.0, 0.1, 0.3$ and $c = -3.13 \times 10^{-34}$ J.

as 0.5 as an example. Figure 4(a) plots the final value of s_0 at $B_0 = 2$ G, i.e. s_0^{Final}, for different sweep rates of the magnetic field. The plot suggests that our discussions on spin tunnelling can be divided into three parts according to the various values of the sweep rates α.

(a) When $\alpha \rightarrow 0$, s_0^{Final} almost equals the initial condition $s_0^{\text{Initial}} = 0.5$, as if the system has not been changed. The plot of tunnelling probability versus sweep rate is almost a line, which indicates that no tunnelling occurs after the external magnetic fields sweep slowly from -2 G to 2 G. In this case, the system is believed to change adiabatically with the slowly sweeping magnetic field. When the magnetic field changes from -2 to 2 G, δ (the Zeeman shift) changes from an initial value to zero, then returns back to its initial value because of its symmetric dependence on the field (shown in figure 1). Hence, the classical Hamiltonian (5) comes back to the origin, although the field has changed dramatically. Numerically solving equations (6) and (7) (also see the phase space figure 6) gives the result that, for a fixed magnetic field, the motions are periodic. Hence, in the light of adiabatic theory [23], if the sweep rate of the external magnetic field is small compared to the frequencies of the instantaneous periodic orbits, the system undergoes adiabatic evolution. Therefore, $s_0^{\text{Final}} \approx s_0^{\text{Initial}}$.

(b) When $\alpha \rightarrow \infty$, s_0^{Final} also tends to 0.5 (its initial value). The final value of s_0 oscillates around 0.5 and tends to a line. In this case, the sweep rate is so quick that the system (5) is restored quickly. The time of change for the magnetic field is much shorter than the period of motion of the system. It is expected that there is no time for the system to give some response to the change in field. So, no tunnelling phenomenon for a very fast sweep rate can be well understood.

(c) Interesting phenomena emerge when α is moderate. For this case, we find that s_0^{Final} changes dramatically with sweep rate, indicating that spin tunnelling occurs, and that the tunnelling probability is sensitive to the sweep rate and the plots are resolvable at a resolution of 10^{-4} G s^{-1}
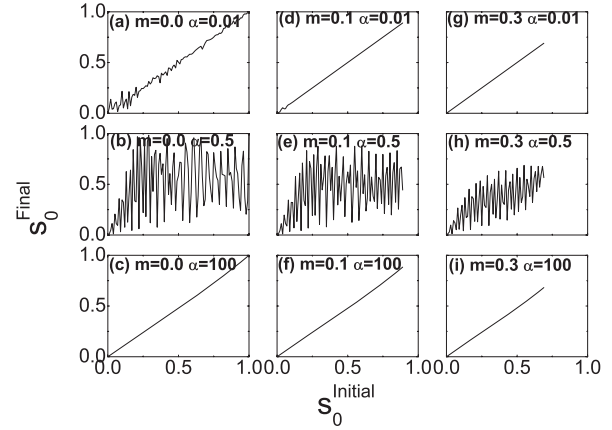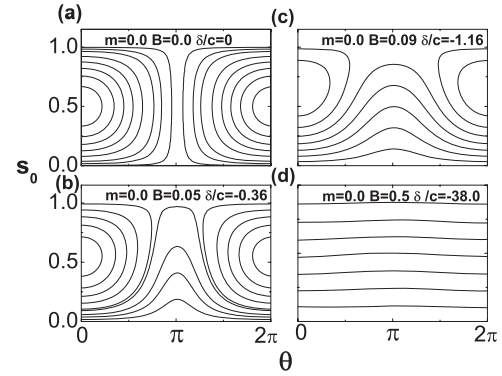

Figure 6. The phase space of ^{87}Rb for different magnetic fields B at $c = -3.13 \times 10^{-34}$ J, $m = 0.0$. The unit of B is Gauss.

of α. In figures 4(b)–(d) we plot the magnifying part of figure 4(a) around $\alpha = 1.55$, which demonstrates this sensitivity.

All the above spin tunnelling phenomena are general and independent on the initial condition. To comprehend this point of view more clearly, we investigate the relationship between s_0^{Initial} and s_0^{Final}. In figure 5, we take $\alpha = 0.01, 0.5, 100$ and calculate the relationship between s_0^{Initial} and s_0^{Final} for several m. It is a smoothly diagonal line for $\alpha = 0.01$ and 100, which stands for no tunnelling occuring. At $\alpha = 0.5$, sensitive tunnelling occurs. For fixed α, the larger the value of m, the smoother the line is, which indicates that m suppresses irregular tunnelling (also see figure 2). This indicates that, for an arbitrarily initial condition, spin tunnelling properties are similar to the above findings. For example, for $s_0^{\text{Initial}} = 1.0$, after a round sweep of the external magnetic field, figures 5(a) and (c) show that the corresponding s_0^{Final} is about 1.0 for adiabatic conditions and a fast sweep condition, e.g. no tunnelling. Figure 5(b) shows that the corresponding s_0^{Final} is no longer equal to the initial condition for moderate sweep conditions, e.g. tunnelling occurs.
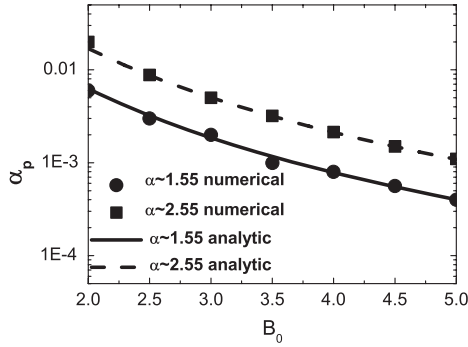
Figure 7. The relationship between α_P and B_0 around $\alpha = 1.55$ and $\alpha = 2.55$. The dots and the squares are numerical results. The solid line and the dashed line are analytical results. The vertical axis is the logarithm.

3.3. Theoretical interpretation for the sensitivity of spin tunnelling on the sweep rate

In this subsection, we achieve insight into the irregular spin tunnelling effect of spinor BECs with the phase space of the classical Hamiltonian H_c [25] and theoretical analysis. We give some interpretations for the sensitivity of the spin tunnelling on the sweep rate observed in the above.

Figure 6 plots the phase space of the Hamiltonian (5) for ^{87}Rb for different values of δ/c. In this phase space we can find two different dynamical regions: (I) a running phase region, where the relative phase θ varies monotonically in time; (II) an oscillating phase region, where θ oscillates in time around a fixed point. When δ/c varies, the areas of these two regions change. In particular, outside the resonance window, the phase space is full of horizontal lines, as demonstrated by figure 6(d), showing that the relative phase θ varies in time linearly for a fixed magnetic field, and that the population of the spin-0 state stays constant almost. On sweeping the field, the phase θ accumulates until the magnetic field gets into the resonance window around $B = 0$, where a jump emerges, as seen in figure 2. The total phase accumulated in the process determines the jump height and therefore affects the final tunnelling probability. The phase accumulation relies on the sweep rate as well as on the initial magnetic field. To demonstrate this, let us suppose that the jump occurs at zero field. From equation (7), we only consider the first term of its right-hand side, which is believed to give the main contribution to the phase change. By making the Taylor expansion of δ around $B = 0$, we find a square relation between δ and the instantaneous field B, i.e. $\delta \approx \rho B^2$, where

$$\rho = \frac{g_I^2 \mu_I^2}{16 E_{hf}} + \frac{g_I \mu_I g_J \mu_B}{8 E_{hf}} + \frac{g_J^2 \mu_B^2}{16 E_{hf}}. \qquad (8)$$

Then we obtain the phase accumulation,

$$\theta_1 = -\frac{2}{3\hbar} \rho \alpha_1^2 t_1^3 = -\frac{2\rho B_0^3}{3\hbar \alpha_1}, \qquad (9)$$

where α_1 is the sweep rate and t_1 is the time during which the magnetic field sweeps from $-B_0$ to 0. Now we consider another field of a slightly different sweep rate α_2, sweeping
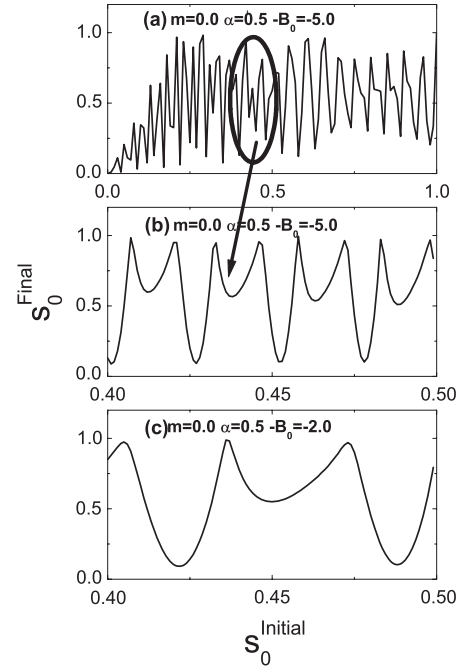

Figure 8. The magnified part of the relationship between s_0^{Initial} and s_0^{Final} around $s_0^{\text{Initial}} = 0.4$ at $m = 0.0$, $c = -3.13 \times 10^{-34}$ J in a moderate swept magnetic field, i.e. $\alpha = 0.5$: (a) is at $-B_0 = -5.0$ G; (b) and (c) are magnified graph of (a) at $-B_0 = -5.0$ G and $-B_0 = -2.0$ G, respectively.

from $-B_0$ to 0. The difference in total phase accumulation between the two processes is estimated as,

$$\Delta\theta = \theta_2 - \theta_1 = \frac{2\rho}{3\hbar} \left(\frac{B_0^3}{\alpha_1} - \frac{B_0^3}{\alpha_2} \right). \qquad (10)$$

Then, we can estimate the inherent period α_p of the tunnelling probability versus the sweep rate in figure 4(d) from the above expression by setting $\Delta\theta = 2\pi$:

$$\alpha_p = \frac{3\Delta\theta \hbar \alpha^2}{2\rho B_0^3}. \qquad (11)$$

The above analysis is confirmed by our numerical calculations. In figure 7, we plot the relationship between α_P and B_0 around $\alpha = 1.55$ (the dots) and $\alpha = 2.55$ (the squares). We find that they agree very well with the results of formula (11). From this formula, we also see a square relation between α_p and the sweep rate. This implies the sensitivity of the spin tunnelling probability on the sweep rate (figure 4).

Actually, for a moderate sweep rate, the sensitive relationship between s_0^{Initial} and s_0^{Final} in figure 5 is also explained by the above argument, that is, when the resolution of the values of s_0^{Initial} is increased, the periodic patterns are obvious. Figure 8 shows a magnified part of figure 5 around $s_0^{\text{Initial}} = 0.4$. Figures 8(b) and (c) plot this kind of periodic structure for different initial magnetic fields. To account for this, similar to the above discussions, the second term in the right-hand side of equation (7), which is believed to give a main contribution to the phase change, is considered. We obtain

$$\theta_1' = -\frac{8c}{\hbar} s_{01} t = -\frac{8c s_{01} B_0}{\hbar \alpha}, \qquad (12)$$
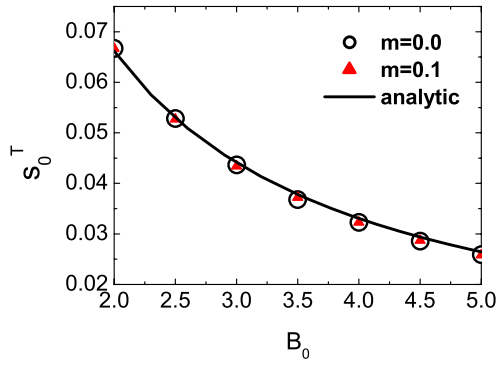
Figure 9. The relationship between s_0^T and B_0 around $s_0^{Initial} = 0.4$. The circles and the triangles are numerical results for $m = 0.0, 0.1$ respectively, and $\alpha = 0.5$. The solid line is the analytical result.
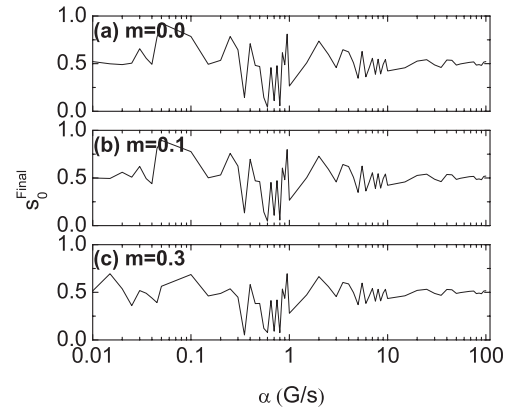

Figure 10. The tunnelling probability of ^{23}Na for $m = 0.0, 0.1, 0.3$ at $c = 3.13 \times 10^{-34}$ J in the swept magnetic field.

where s_{01} is an initial value of spin zero population and t is the time during which the magnetic field sweeps from $-B_0$ to 0. For the same sweep rate α, we consider another initial value of spin zero population, i.e. s_{02}. In the two processes, the difference in the total phase accumulation is estimated to be

$$\Delta\theta' = \theta'_2 - \theta'_1 = -\frac{8cB_0}{\hbar\alpha}(s_{02} - s_{01}). \tag{13}$$

Then, the period of the regular structure in figure 8 is estimated as

$$s_0^T = -\frac{\Delta\theta'\hbar\alpha}{8cB_0}, \tag{14}$$

where $\Delta\theta' = 2\pi$. In figure 9, the above formula (14) is confirmed by our numerical simulations. We see that the analytical result agrees very well with the numerical calculation. Besides, we find that the above relation is independent of m.

4. ^{23}Na atom condensate

^{23}Na atom condensate has also been prepared in experiments, and its dynamics are also interesting. In contrast to ^{87}Rb, the interaction between ^{23}Na atoms is attractive. In this section, we discuss the spin tunnelling of ^{23}Na. First, we still take the initial probability of s_0 to be 0.5 in order to compare with ^{87}Rb atom condensate. As in the above section, our discussions are divided into three parts according to the values of the sweep rate α. The main results are shown in figure 10. We see that the tendencies of the tunnelling probability of ^{23}Na atoms are the same as those of ^{87}Rb atoms. Two little differences are found by comparing the two atom condensates.

The first difference is the adiabatic range. For the ^{23}Na system, the adiabatic range is smaller than that of the ^{87}Rb system. Because the frequencies of the instantaneous periodic orbits of the ^{23}Na atom system are smaller than those of the ^{87}Rb condensate, the ^{23}Na system needs a smaller sweep rate to satisfy the adiabatic condition. This difference does not affect the fact that no tunnelling occurs with $\alpha \to 0$. When $\alpha \to \infty$ and α is moderate, the tunnelling phenomena of the ^{23}Na system are similar to the counterparts of the ^{87}Rb atom system.
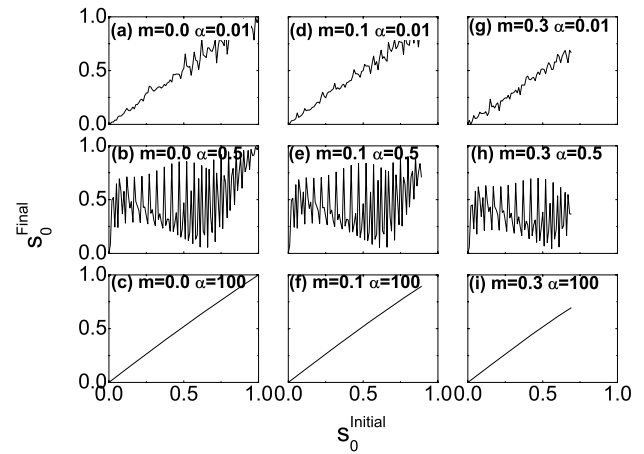

Figure 11. The relationship between $s_0^{Initial}$ and s_0^{Final}, for $\alpha = 0.01, 0.5, 100$, $m = 0.0, 0.1, 0.3$ and $c = 3.13 \times 10^{-34}$ J.

The second difference is the effect of the conservation m. As for the ^{87}Rb atom condensate, the relationship between s_0^{Final} and $s_0^{Initial}$ is studied to more clearly understand the sensitive spin tunnelling of ^{23}Na atom condensate. Using the same values of α and m as those in the ^{87}Rb atom system, we get the results of s_0^{Final} with $s_0^{Initial}$, as shown in figure 11. When the sweep rate is small, comparing figure 11 with figure 5, we see that the lines in figure 5 are smoother than those in figure 11 for the same α, such as figures 5(d) and 11(d). This indicates that the effect of the conservation m on the spin tunnelling of the ^{23}Na system is less important. When α is moderate, a finite value of m suppresses the amplitude of the tunnelling probability in figures 11(b), (e) and (h) as well as in figures 5(b), (e) and (h). The difference is the amplitude of the fluctuation. The suppression effect of the finite magnetization m on the sensitivity of the tunnelling probabilities for the ^{23}Na system is less significant than that for the ^{87}Rb system. When α is larger, i.e. in the sudden limit, figures 11(c), (f) and (i) show identical smooth lines without any fluctuations, as in figures 5(c), (f) and (i).

As discussed above, the tunnelling phenomena for the ^{23}Na and ^{87}Rb atom condensates have no essential differences.

So it is not necessary to repeat the interpretation for sensitive spin tunnelling in the ^{23}Na system.

5. Conclusion

In conclusion, we have investigated the tunnelling dynamics of a spin-1 Bose–Einstein condensate in a linearly swept magnetic field theoretically within the framework of mean-field treatment. We focus on the two typical alkali Bose atoms ^{87}Rb and ^{23}Na condensates and study their tunnelling dynamics according to different sweep rates of external magnetic fields. In particular, we find that the spin tunnelling probability is very sensitive to the sweep rate in a certain parameter regime. With the help of both analytical deductions and phase space analysis, we have given a complete explanation for the above finding. In addition, we have investigated the effect of the conserved magnetization on the dynamics of the spin tunnelling.

All the above findings can be observed with the present experimental technique. As in [13], the atoms are loaded directly from a magneto-optical trap into an optical dipole force trap formed by a CO_2 laser. Lowering the laser power forces evaporative cooling in the optical trap, leading to rapid condensation. With different magnetic field gradients during the evaporation process, the initial spin population could be controlled. Beginning with pure spin-0 condensates as the initial condition, i.e. $s_0^{\text{Initial}} = 0.5$, differing from [13] where a fixed external magnetic field is used, we sweep the field from -2 to 2 G at a given sweep rate. After the sweep, the spin populations are measured by using absorptive imaging. So, we believe that our studies can stimulate the experimental study of spinor BECs.

Acknowledgments

References

[1] Regal C A, Greiner M and Jin D S 2004 *Phys. Rev. Lett.* **92** 040403
[2] Zwierlein M W, Stan C A, Schunck C H, Raupach S M F, Kerman A J and Ketterle W 2004 *Phys. Rev. Lett.* **92** 120403
[3] Matthews M R, Anderson B P, Haljan P C, Hall D S, Wieman C E and Cornell E A 1999 *Phys. Rev. Lett.* **83** 2498
[4] Madison K W, Chevy F, Wohlleben W and Dalibard J 2000 *Phys. Rev. Lett.* **84** 806
[5] Raman C, Abo-Shaeer J R, Vogels J M, Xu K and Ketterle W 2001 *Phys. Rev. Lett.* **87** 210402
[6] Greiner M, Mandel O, Esslinger T, Hänsch T W and Bloch I 2002 *Nature* **415** 39
[7] Olshanii M 1998 *Phys. Rev. Lett.* **81** 938
[8] Görlitz A, Vogels J M, Leanhardt A E, Raman C, Gustavson T L, Abo-Shaeer J R, Chikkatur A P, Gupta S, Inouye S, Rosenband T and Ketterle W 2001 *Phys. Rev. Lett.* **87** 130402
[9] Myatt C J, Burt E A, Ghrist R W, Cornell E A and Wieman C E 1997 *Phys. Rev. Lett.* **78** 586
[10] Stenger J *et al* 1998 *Nature* **396** 345
[11] Miesner H-J *et al* 1999 *Phys. Rev. Lett.* **82** 2228
[12] Stamper-Kurn D M *et al* 1999 *Phys. Rev. Lett.* **83** 661
[13] Chang M-S, Hamley C D, Barrett M D, Sauer J A, Fortier K M, Zhang W, You L and Chapman M S 2004 *Phys. Rev. Lett.* **92** 140403
[14] Diener R B and Ho T-L 2006 *Phys. Rev. Lett.* **96** 190405
[15] Stamper-Kurn D M *et al* 1998 *Phys. Rev. Lett.* **80** 2027
[16] Barrett M, Sauer J and Chapman M S 2001 *Phys. Rev. Lett.* **87** 010404
[17] Ohmi T and Machida K 1998 *J. Phys. Soc. Japan* **67** 1822
[18] Ho T-L 1998 *Phys. Rev. Lett.* **81** 742
[19] Law C K, Pu H and Bigelow N P 1998 *Phys. Rev. Lett.* **81** 5257
[20] Pu H, Law C K, Raghavan S, Eberly J H and Bigelow N P 1999 *Phys. Rev.* A **60** 1463
[21] Zhang Wenxian, Zhou D L, Chang M-S, Chapman M S and You L 2005 *Phys. Rev.* A **72** 013602
[22] Pethick C J and Smith H 2002 *Bose–Einstein Condensation in Dilute Gases* (Cambridge: Cambridge University Press) chapter 3
[23] Liu J, Wu B and Niu Q 2003 *Phys. Rev. Lett.* **90** 170404
[24] Wang G-F, Ye D-F, Fu L-B, Chen X-Z and Liu J 2006 *Phys. Rev.* A **74** 033414
[25] Wang G-F, Fu L-B and Liu J 2006 *Phys. Rev.* A **73** 013619